2D Inversion of Self Potential Data

Dissertation report Submitted in

partial fulfillment of the requirements of

the degree

of

M.Sc. Applied Geophysics

by

Madhusudan Sharma

Supervisor**:**

Prof. Anand Singh

Department of Earth Sciences

Indian Institute of Technology Bombay

2021-2023

Approval Sheet

The M.Sc. dissertation entitled "**2D-Inversion of Self Potential data**" prepared by Madhusudan Sharma (Roll No.-215320003) is hereby approved for final submission.

Prof.K.H.Singh   **Prof.B.Shekhar**   **Prof.Anand Singh**

(Examiner)   (Examiner)   (Supervisor/Examiner)

Declaration

I declare that this written submission represents my ideas in my own words and where others' ideas or words have been included, I have adequately cited and referenced the original sources. I also declare that I have adhered to all principles of academic honesty and integrity and have not misrepresented or fabricated or falsified any idea/data/fact/source in my submission. I understand that any violation of the above will be cause for disciplinary action by the Institute and can also evoke penal action from the sources which have thus not been properly cited or from whom proper permission has not been taken when needed.

. . . .
27 April 2023

. . . .
Madhusudan Sharma
Roll no. 215320003
M.Sc. Applied Geophysics

Table of Contents

Acknowledgement

List of Figures

Abstract

This report details the application of inversion techniques to self potential data collected in the Ambet region near Mumbai, with the aim of identifying potential water bodies in the subsurface. The report discusses the methods used for data acquisition and processing, as well as the compact inversion algorithms employed. The results of the inversion are presented and interpreted, highlighting potential locations of water bodies in the subsurface. The report concludes witha discussion of the significance of these findings and potential areas for future research.

Keywords: Self potential, Source inversion.

Chapter 1

Introduction

1.1 Self potential method

Self-potential (SP) measurements are a non-invasive geophysical method that involves measuring the electrical potential differences between points on the ground surface. SP measurements can provide information on subsurface electrical conductivity and can be used to locate and map subsurface geological features such as mineral deposits, faults, and groundwater reservoirs.

The origin of self-potential signals is due to several natural and man-made processes. In general, self-potential signals are created by the flow of electrical charges within the earth's subsurface, resulting from electrochemical or mechanical actions. The electrochemical actions can be attributed to the differences in the chemical composition of subsurface fluids such as groundwater, which creates potential differences between the fluids and the surrounding rock matrix . The mechanical actions can arise from the deformation of the subsurface, which generates electrical currents due to the relative motion between minerals with different conductivities. Additionally, man-made disturbances such as buried electrical cables, drainage pipes, or waste disposal sites can also generate SP signals, which can be important in the study of environmental problems.

1.2 Workflow

The workflow for this study involves several steps, starting with the collectionof self-potential data and DC resistivity data from the Ambet region. The primary focus of the study is to use source inversion techniques to identify potential water bodies in the subsurface. The following outlines the workflow in more detail:

1. Data Collection: The first step is to collect self-potential and DC resistivity data from the Ambet region. The self-potential data is collected using potential and reference electrodes placed on the ground surface. The DC resistivity data is collected using an array of electrodes to measure the electrical resistance of the subsurface.

2. Forward Modelling: In this step, we use the subsurface resistivity information obtained from the DC resistivity data to perform forward modelling.The forward modelling involves simulating the self-potential signals that would be expected based on the subsurface resistivity and source information.

3. Inversion: In the final step, we perform inversion on the self-potential data to identify the source of current in the subsurface. The inversion processinvolves solving a mathematical equation that relates the self-potential datato the source of current in the subsurface. The resulting inversion model provides information on the location and size of potential water bodies inthe subsurface.

In summary, the workflow for this study involves collecting self-potential and DC resistivity data, performing forward modelling to obtain a theoretical modelof the subsurface, and using inversion techniques to identify the source of cur-rent in the subsurface and potential water bodies in the Ambet region.

Chapter 2

Instrumentation and field measurement

2.1   Self Potential field equipment

The origin of the SP method can be traced back to 1830 when Robert Fox employed copper-plate electrodes and a string galvanometer as a detector to explore the extension of underground copper deposits in Cornwall. Since 920, this method has been used as a secondary approach for base metal search. The equipment required for this technique is relatively simple, comprising a pair ofelectrodes connected by wire to a millivolt meter. However, there are two crucial restrictions related to the electrodes and detector. If metal stakes are used as SP electrodes and driven into the ground, they can generate electrochemical reactions at the ground contact, resulting in spurious potential measurementsof the same magnitude as those being measured. Additionally, these contact potentials may vary widely in different ground conditions and at different times, making it difficult to correct them accurately. Consequently, nonpolarised electrodes are essential for accurate measurements. These electrodes consist of a metal immersed in a saturated solution of its own salt, such as Cu in $CuSO_4$ or Ag in AgCl, and are contained in a porous pot that permits the solution toleak slowly and make contact with the ground. A walking stick arrangement shown in Figure 2.1 is an example of a good nonpolarising electrode for the SP method.
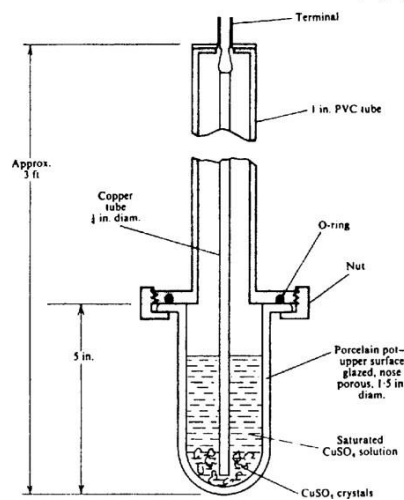
Figure 2.1: Walking stick SP electrode

The primary requirement for the millivolt meter is that its input impedance should be large enough to draw negligible current from the ground during the measurement. In the past, this was achieved by using a potentiometer, but nowadays, a small digital DC meter with an input impedance greater than 10^8 ohm is readily available. Such instruments have a range from 10 mV to 20 Vfull scale. To prevent erratic readings caused by contact of the instrument casewith the body or ground, it is sometimes necessary to enclose the meter in a shield can.

2.2 Field measurement

To ensure accurate readings, it is recommended that both porous pots are filled with a uniform batch of salt solution. Alternatively, the pots can be partly filled with salt crystals and water, but the first method is preferred. Once loaded, the pots should be placed next to each other in a hole in the ground and connected to a meter. Ideally, the reading should be less than 2 mV. If the reading is higher, the pots should be cleaned and recharged with fresh solution.

Typically, the pots can be used for a few days before running dry.

When conducting traverses to investigate suspected SP anomalies, it is bestto traverse normal to the strike. Station intervals should be no greater than 30m and may be as small as 3 m. One electrode is fixed at the base station, while the other moves to successive stations along the line. Alternatively, bothelectrodes can be moved while maintaining a fixed interval between them. Thefirst arrangement, recommended for long traverses, requires a reel with severalkilometers of cable. The meter may be located at either electrode, but it is usually at the base station.

The advantage of this layout is that the potential is continuously measured with respect to a fixed point, preferably in a barren area. Additionally, small zero errors between the electrodes do not accumulate. The only disadvantage isthe long cable, which can slow down the measurement process.

2.3   Field Region

In this project I performing inversion of Ambet region Self-potential data. The Ambet region is located in the Raigad district of Maharashtra, India, approximately 60 km east of Mumbai. Geologically, the region is part of the Deccan Traps, which is a large volcanic province that covers most of central India. The Deccan Traps were formed during the late Cretaceous period around 65 millionyears ago, when the Indian subcontinent was moving northward and encountereda hot spot in the Earth's mantle. This caused a massive outpouring of lava that covered an area of around 500,000 square kilometers, resulting in the formationof a large igneous plateau.

In the Ambet region, the volcanic rocks are primarily composed of basalt,

(a)

Figure 2.2: **Map showcasing the geographical area of Ambet's study region**

which is a dark-colored, fine-grained igneous rock. The basalt flows in the area are usually horizontally layered and can be several meters thick. The region also contains a variety of volcanic structures such as lava tubes, which are formed when lava flows underground and forms a hollow tube.

In Fig. 2.3a a contour plot is displayed along with Profile 1 and Profile2, on which we are taking self-potential and DC resistivity data. Additionally, Fig. 2.3b presents self-potential data.

In Fig. 2.4a and Fig. 2.4b both show the DC resistivity data of Profile 1 and Profile 2, respectively.
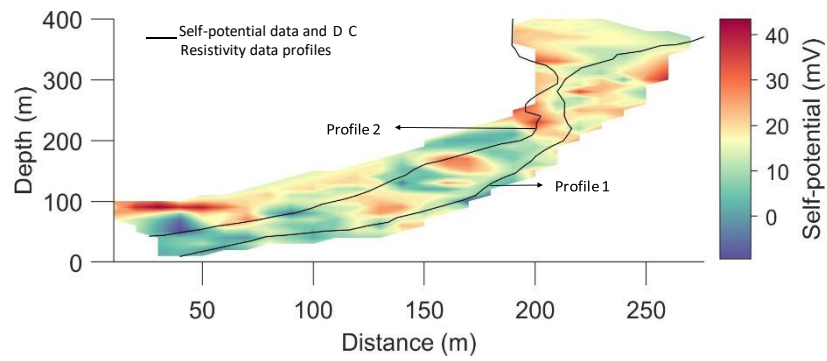
(a)
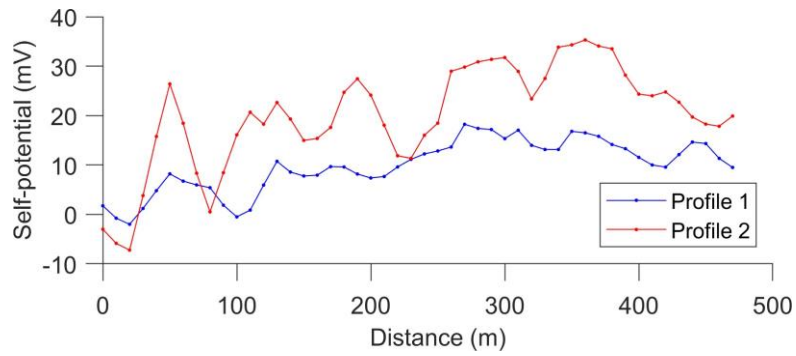
(b)

Figure 2.3: **(a) A contour plot visualizing data and providing insights into profiles visualization. (b) Self potential data plots for profile 1 and 2**

Figure 2.4: (a) Apparent resistivity data of profile 1 (b) Apparent resistivity data of profile 2.

Chapter 3

Modelling and Inversion of Self-Potential data

We collect two types of data from the same field region: apparent DC resistivity data and self-potential data. Once we have gathered all t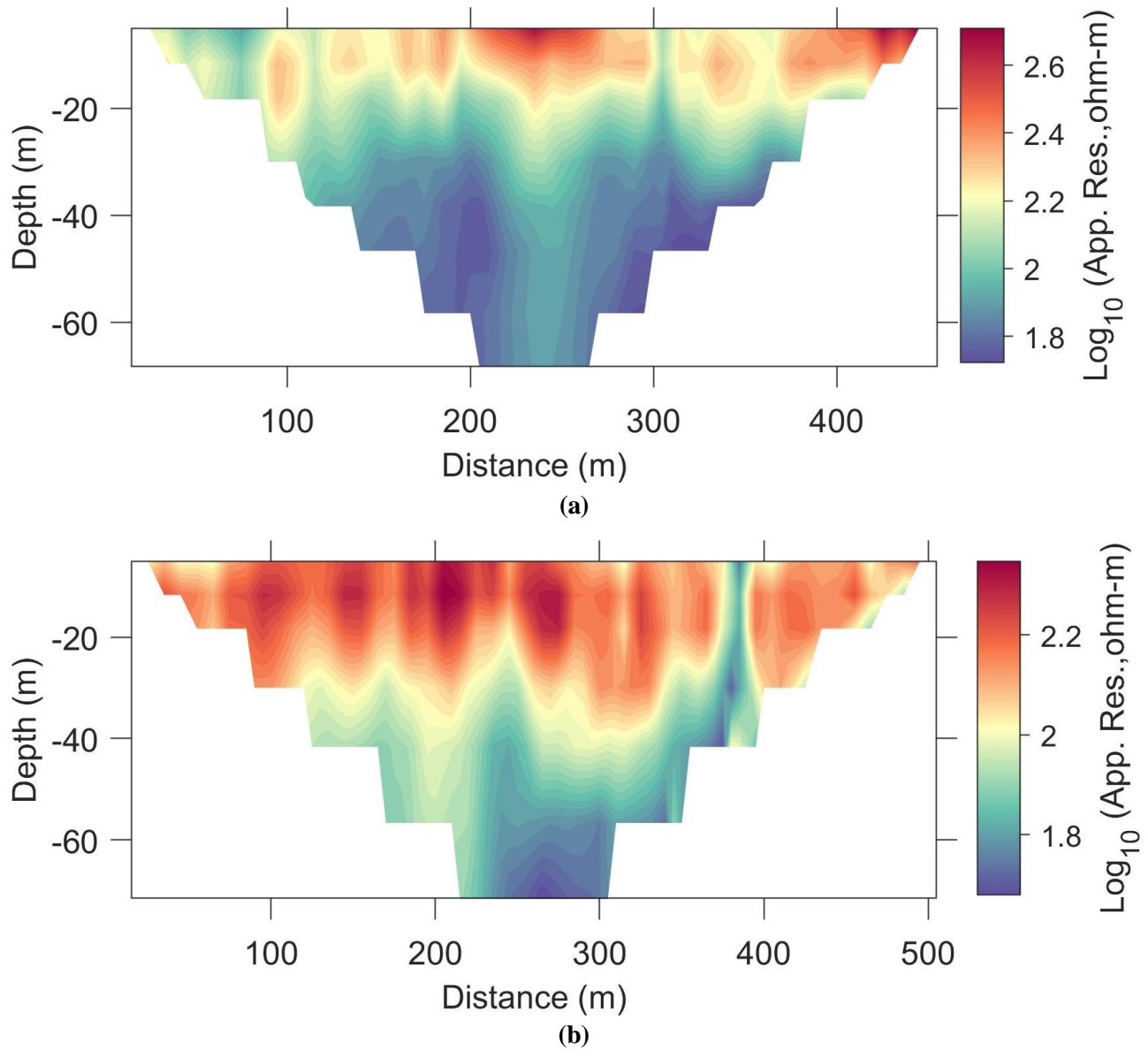he data, our first processing step involves conducting a DC inversion to obtain a conductivity model of the subsurface. This model provides us with information about the conductivity of the region. Next, we calculate the self-potential by placing a source in the subsurface. When the self-potential is close to the observed data, we fix the G and use it for further inversion. DC electrical response dueto source in a conductive medium is
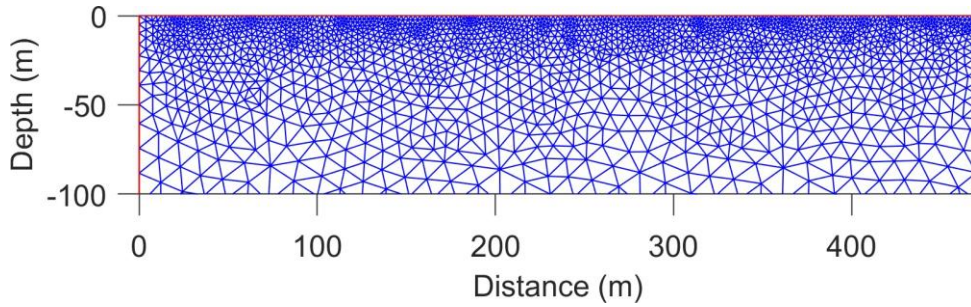
$$\nabla \cdot \sigma \nabla \varphi = s \qquad (3.1)$$

3.1   Finite element method

When using a triangular grid to discretize the Poisson equation with FEM, the following steps are typically involved:

1. Mesh generation: The region of interest is divided into a mesh of tri-
   angles, with each triangle defined by three nodes. The vertices of the

Figure 3.1: Triangular mesh grid.

triangles are shared by neighboring triangles, which allows us to build a connected mesh.

2. Basis functions: We use a piecewise linear function to approximate the solution over each triangle. These basis functions are chosen to satisfy certain properties, such as being continuous and differentiable over the tri- angle boundaries. One example of a basis function used in self-potential (SP) method with finite element method (FEM) is the linear hat function.This function is defined over each triangular element of the mesh and hasthe following form:

$$\varphi(x, y) = c1 + c2 * x + c3 * y \tag{3.2}$$

where c1, c2, and c3 are constants determined by the nodal values of the function at the three vertices of the triangle.

To illustrate this, consider a triangular element with vertices (x1, y1), (x2, y2), and (x3, y3), and let φ 1, φ 2, and φ 3 be the nodal values of the basis function at these vertices. Then, we can determine the coefficients

c1, c2, and c3 as follows:

$$c1 = \varphi 1$$

$$c2 = (\varphi 2 - \varphi 1)/(x2 - x1) + (\varphi 3 - \varphi 1)/(x3 - x1)$$

$$c3 = (\varphi 2 - \varphi 1)/(y2 - y1) + (\varphi 3 - \varphi 1)/(y3 - y1)$$

Once we have the coefficients c1, c2, and c3, we can evaluate the basis function at any point (x,y) within the triangular element using the above equation.

3. Weak formulation: We use the Galerkin method to obtain a set of linear equations that relate the nodal values of the solution to the source term and boundary conditions. These equations are derived by enforcing the Poisson equation over each triangle.

4. Assembly: The equations obtained for each triangle are assembled into a global system of equations that can be solved using numerical methods.

5. Solution: The resulting system of equations is sparse, which means that most of the coefficients are zero. This allows us to use specialized sparse matrix algorithms to solve the system efficiently. Once the nodal values are obtained, we can interpolate the solution over the entire region using the nodal values and the piecewise linear basis functions.

After discretizing Poisson equation using finite element method we rearranged for calculated self-potential and get G.

$$Gs = \varphi_d^{cal} \tag{3.3}$$

where φ_d^{cal} is calculated potential at measurement locations. Once we have fixed G, we can perform inversion to obtain the source of the real subsurface which is our next step.

3.2   Inversion

The compact inversion principle, as proposed by Last and Kubik in 1983, involves minimizing the size of the source body while maximizing its compact- ness. In cases where the problem is slightly underdetermined, the weighted- damped least-squares method is used to solve the inversion problem.

$$s = W_v^{-1} G^T (G W_v^{-1} G^T + W_e^{-1})^{-1} \varphi_d^{obs} \tag{3.4}$$

Where W_v is current density weighting matrix. Initially we take W_e and W_v as identity matrix.

$$W_v^{-1} = (s)^2 + \beta \tag{3.5}$$

β is perturbation number and for this project we kept it 10^{-12}.

$$W_e^{-1} = N/S diag(G W_v^{-1} G^T) \tag{3.6}$$

Where W_e is noise weighting matrix is an a posteriori covariance matrix that depends on the current density weighting matrix, the kernel, and a parameter that states the priori estimated noise to signal ratio N/S.

This method consist of an iterative procedure in which the weighting matrices change at each iteration until satisfying convergence of the solution is obtained. The model resolution is greatly affected by the choice of the parameter N/S. High values mean that the inversion result is more compact, while lowvalues mean that the inversion procedure fits the data better. The choice of theiteration that offers the best fitting is determined by the minimum norm between calculated and experimental data. A "mask signal" approach is proposed, which involves evaluating the signal power spectrum in the wave number domain, estimating the k-numbers, evaluating the running signal power along the survey line, choosing an energy threshold between the "useful signal" and the noise, and determining the segments where the main anomalies are located. This approach allows the inversion operator to focus on those parts of the signal thatcarry information on the targets. Figure 3.2 represent flowchart of self-potential inversion for better understanding.
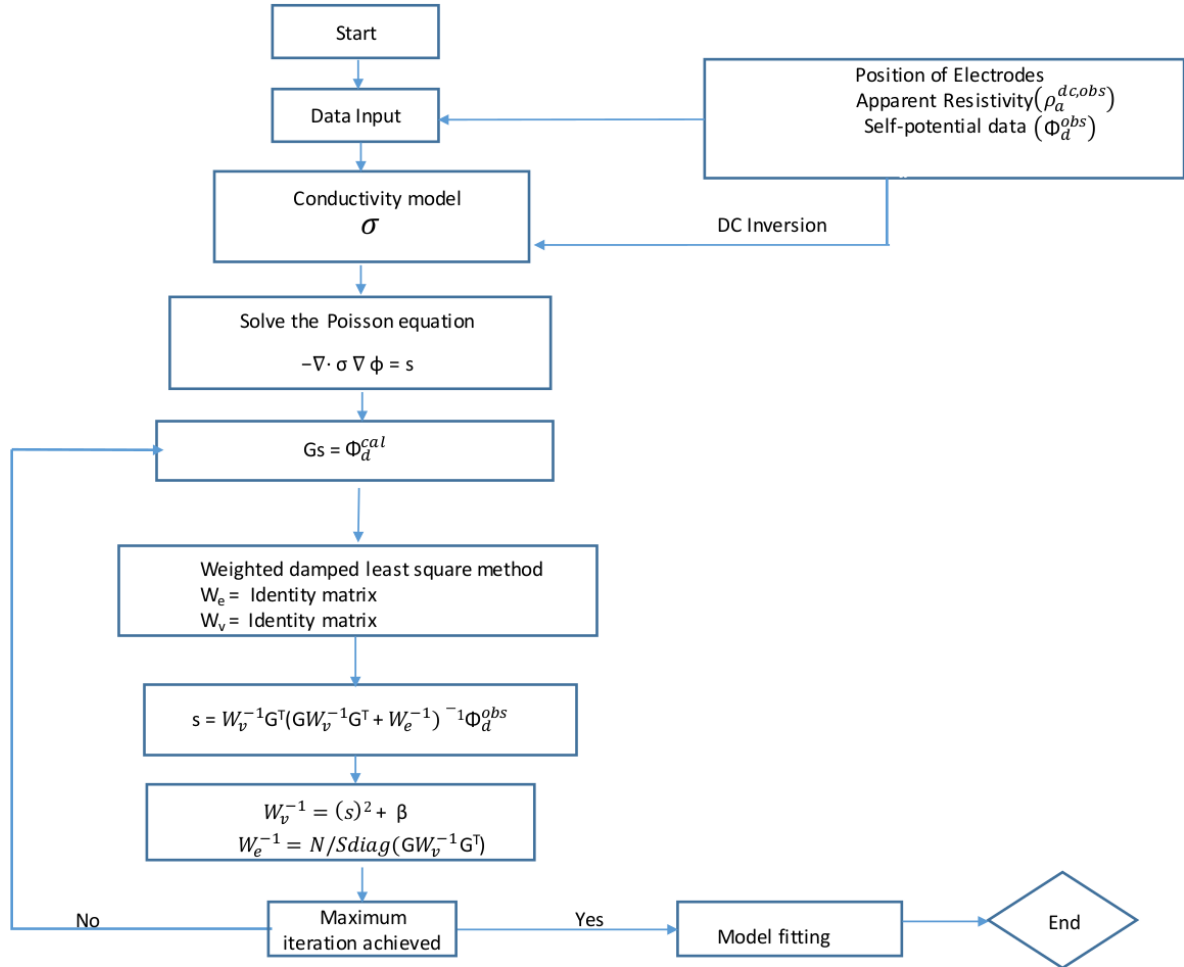
Figure 3.2: Flowchart of inversion of self-potential data.

The flowchart contains the following elements:

- Start
- Data Input
- Position of Electrodes, Apparent Resistivity $(\rho_a^{dc,obs})$, Self-potential data (Φ_d^{obs})
- Conductivity model σ
- DC Inversion
- Solve the Poisson equation $-\nabla \cdot \sigma \nabla \phi = s$
- $Gs = \Phi_d^{cal}$
- Weighted damped least square method, W_e = Identity matrix, W_v = Identity matrix
- $s = W_v^{-1}G^T(GW_v^{-1}G^T + W_e^{-1})^{-1}\Phi_d^{obs}$
- $W_v^{-1} = (s)^2 + \beta$, $W_e^{-1} = N/Sdiag(GW_v^{-1}G^T)$
- Maximum iteration achieved — No / Yes
- Model fitting
- End

Chapter 4

Results and Conclusion

4.1 Profile 1

The focus of this analysis is on Profile 1, as depicted in Fig. 4.1a. The results obtained from this analysis indicate that there are high potential values observed between approximately 20-60 meters in depth and distances of 200- 300m and 350-400m. Further clarity can be gained by cross-referencing these findings with Fig. 4.1b, which shows high natural source current values in thesame depth and distance ranges. However, the maximum current value observedis only 0.4 mA, which falls below the threshold required to confirm the presence of water flow. Typically, a 14-15 mA is required to validate the existenceof water flow. Fig. 4.1c, which depicts subsurface resistivity, also supports these findings. The combined analysis of these three figures indicates that theremay be some water flow present, but the current values are too low to draw any definitive conclusions.
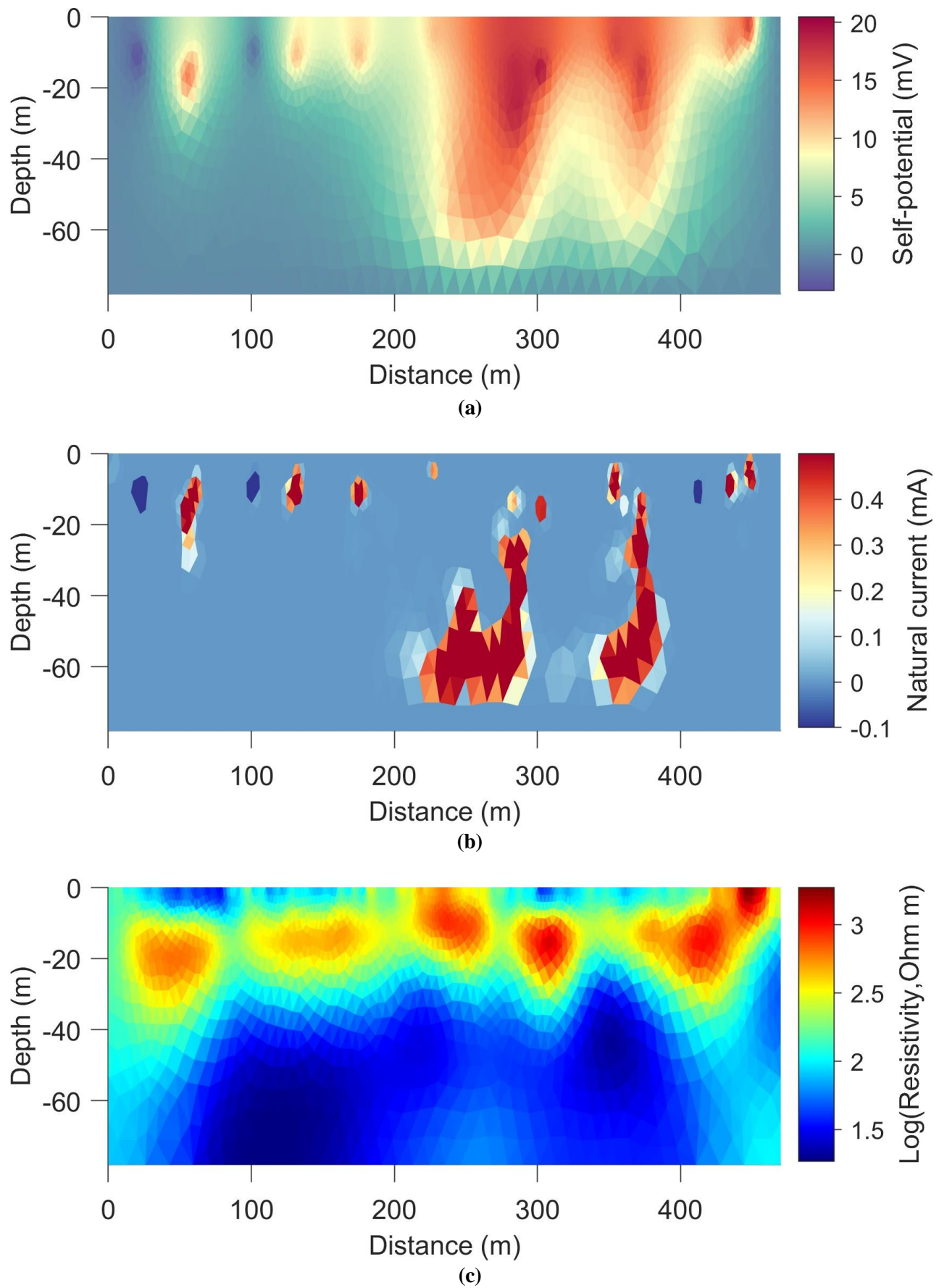
Figure 4.1: **(a) Subsurface self potential data of profile 1. (b) Current density of subsurfac of profile 1. (c) Resistivity of subsurface of profile 1.**

4.2   Profile 2

Within this particular section, our primary focus lies on Profile 2, and its corresponding results, which are exemplified in Figure 4.2. Specifically, within part (a) and part (b), we discovered that high potential nad high natural current values are noticeable at depths ranging between approximately 20-50 meters, and that there are small patches that exist at distances of 250-300m and 350-400m.

In order to obtain additional insight and clarity, we cross-referenced the initial results with Figure 4.2 (c). This supplementary figure demonstrates low resistivity values at the same depth and distance ranges. Despite this, it is important to note that the maximum current value observed only reached 0.4 mA.This measurement falls below the threshold which would be required to confirmthe existence of water flow. In order to validate the existence of water flow, the expected range would typically be between 14-15 mA.

Finally, upon consideration of Figure 4.2 (c), which conveys subsurface resistivity. In combination, these three figures suggest that there may be some presence of water flow, but the current values are not substantial enough to draw any definitive conclusions.

4.3   Sanity check 1

To ensure confidence in our results, we have taken the step of fitting a model with our data. As you can see in Figure 4.3 (a), this has resulted in a good fit between the model and data of Profile 1. We have utilized the minimum norm between the calculated and experimental data for this process.
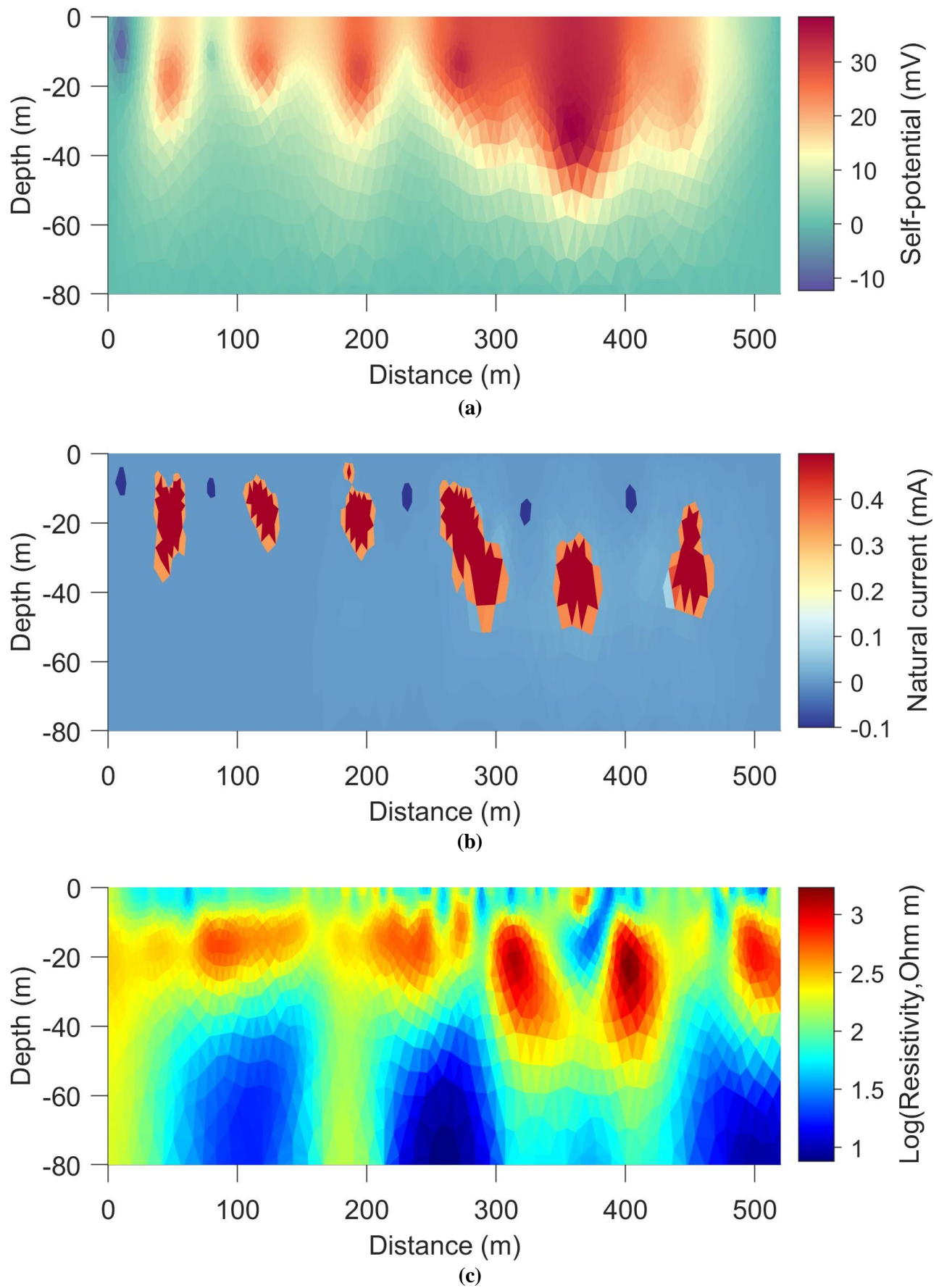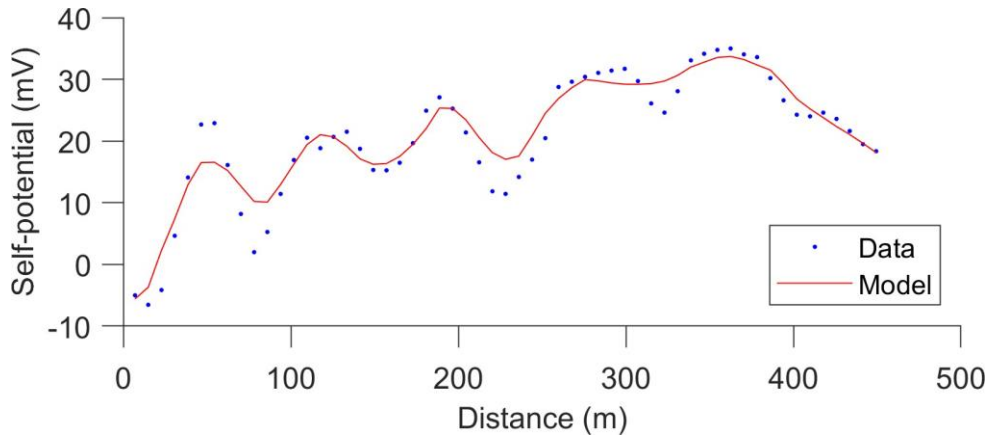
Figure 4.2: **(a) subsurface self potential of profile 2. (b) Current density of subsurface along profile 2. (c)Inverted resistivity section of subsurface along profile 2.**
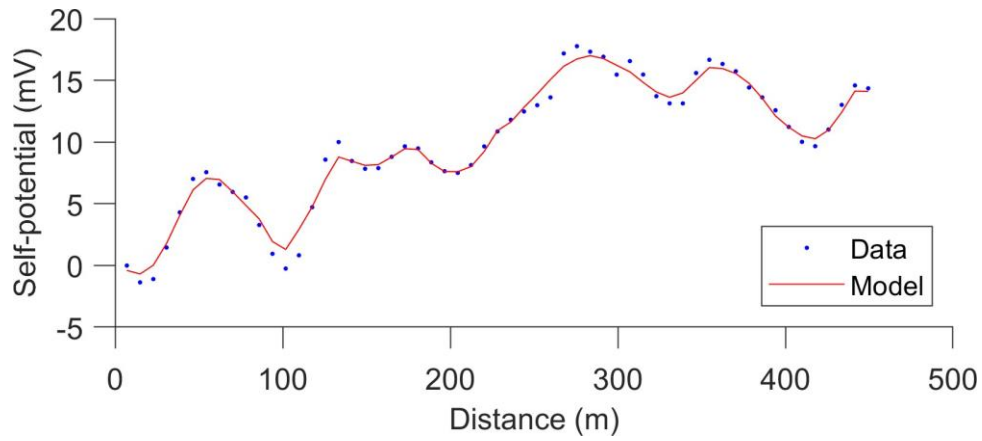
(a)

(b)

Figure 4.3: **(a) Misfit curve of profile 1. (b) Misfit curve of profile 2.**

We have also applied the same fitting procedure to Profile 2. However, in comparison to the first profile, the fitting is not as strong, but it is acceptable for the time being. Our next step involves performing sanity checks 2 and 3, which will include calculating a model resolution matrix, among other measures. By undertaking these additional steps, we aim to validate and reinforce our findings, further solidifying our trust in the accuracy of our results.

4.4   Conclusion

After conducting an analysis of Profile 1 and 2, it appears that there may be a possibility of water flow in the range of 300 to 400 meters distance. However, the low values of natural current do not provide enough confidence to draw definitive conclusions about the presence of water flow. Further investigation is required to confirm the existence of water flow conclusively.

In future studies, collecting data during the rainy season would be beneficial as it would provide more comprehensive information and increase confidence in the conclusive statement.

Reference

A. Revil, A. Finizola, M. Gresse, Self-potential as a tool to assess groundwater flow in hydrothermal systems: A review, Journal of Volcanology and Geother-mal Research, Volume 437, 2023, 107788, ISSN 0377-0273

Burke Minsley. Modeling and inversion of self potential data. 03 2008

K. Key , C. Weiss, GEOPHYSICS, VOL. 71, NO. 6 !NOVEMBER-DECEMBER 2006"; P. G291–G299, 11 FIGS. 10.1190/1.2348091

Last, B.J. and Kubik, K. (1983) Compact Gravity Inversion. Geophysics, 48, 713-721

Laurence Jouniaux, Alexis Maineult, V eronique Naudet, Marc Pessel, and Pascal Sailhac. Review of self-potential methods in hydrogeophysics. Comptes Rendus Geoscience, 341(10):928–936, 2009. Hydrog eophysique.

William Murray Telford, WM Telford, LP Geldart, and Robert E Sheriff. Applied geophysics. 1990

Revil, A., D. Hermitte, M. Voltz, R. Moussa, J.G. Lacas, G. Bourrie, and F. Trolard (2002), Self-potential signals associated with variations of the hydraulichead during an infiltration experiment, Geophys. Res. Lett. , 29 (7), 1106, doi:10.1029/2001GL014294.

Revil, A., H. Schwaeger, L.M. Cathles, and P.D. Manhardt (1999b), Streaming poten- tial in porous media 2. Theory and application to geothermal sys- tems, J. Geo- phys. Res. , 104 (B9), 20033-20048.

S. Stocco, A. Godio, L. Sambuelli, Modelling and compact inversion of magnetic data: A Matlab code, Computers Geosciences, Volume 35, Issue 10, 2009, Pages 2111-2118, ISSN 0098-3004

Sill, W.R. (1983), Self-Potential Modeling from Primary Flows, Geophysics , 48 (1), 76-86.

Silva, J.B.C., W.E. Medeiros, and V.C.F. Barbosa (2001), Potential-field inversion: Choosing the appropriate technique to solve a geologic problem, Geo-physics , 66 (2), 511-520.

Vogel, C.R. (2002), Computational methods for inverse problems, 183 pp., Society for Industrial and Applied Mathematics, Philadelphia.